DALTON
FULL PAPER

X-Ray diffraction and molecular mechanics studies of 12-, 13-, and 14-membered tetraaza macrocycles containing pyridine: effect of the macrocyclic cavity size on the selectivity of the metal ion

Vitor Félix,[a] Judite Costa,[bc] Rita Delgado,[bd] Michael G. B. Drew,[e] Maria Teresa Duarte[df] and Catarina Resende[f]

[a] *Dep. de Química, Universidade de Aveiro, 3810-193 Aveiro, Portugal. E-mail: vfelix@dq.ua.pt*
[b] *Instituto de Tecnologia Química e Biológica, UNL, Apartado 127, 2781-901 Oeiras, Portugal*
[c] *Faculdade de Farmácia de Lisboa, Av. das Forças Armadas, 1600 Lisboa, Portugal*
[d] *Instituto Superior Técnico, Av. Rovisco Pais, 1049-001 Lisboa, Portugal*
[e] *Department of Chemistry, University of Reading, Whiteknights, Reading, UK RG6 6AD*
[f] *Centro de Química Estrutural, Av. Rovisco Pais, 1049-001 Lisboa, Portugal*

Received 6th December 2000, Accepted 19th March 2001
First published as an Advance Article on the web 17th April 2001

The single crystal structures of complexes $[CuL^1Br]ClO_4$ **1**, $[CuL^2Br]PF_6$ **2**, and $[NiL^2][ClO_4]_2$ **3** were determined (L^1 is 3,6,9,15-tetraazabicyclo[9.3.1]pentadeca-1(15),11,13-triene and L^2 is 3,6,10,16-tetraazabicyclo[10.3.1]hexadeca-1(16),12,14-triene). The asymmetric unit of **1** contains two $[CuL^1Br]^+$ cations having different five-co-ordinated environments. One (**A**) exhibits a distorted square pyramidal arrangement, with the basal plane defined by three nitrogen atoms of the macrocycle and the bromine, and the apical position occupied by the nitrogen opposite to the pyridine ring. In the other (**B**) the donor atoms are distorted from this geometry towards a trigonal bipyramid with the equatorial plane formed by two nitrogen atoms of the macrocycle and Br, and the axial positions occupied by the nitrogen atoms contiguous to the pyridine ring. The complex cation $[CuL^2Br]^+$ **2** exhibits a distorted square pyramidal environment with the basal plane defined by the four nitrogen atoms of the macrocycle and the apical co-ordination by the bromine atom. In $[NiL^2]^{2+}$ **3** the four nitrogen atoms of the macrocycle form a distorted square planar environment around the nickel centre. Molecular mechanics calculations are used to determine the best-fit sizes for metal ions accommodated into L^1 and L^2 by evaluation of all sterically allowed conformers for five-co-ordination geometry. The results obtained, together with those of L^3 (3,7,11,17-tetraazabicyclo[11.3.1]-heptadeca-1(17),13,15-triene), published previously, clearly establish the effect of macrocyclic cavity size on metal ion selectivity. These macrocycles prefer a planar conformation to accommodate small metal ions but folded conformations are preferred for longer M–N distances. The increase of the macrocyclic cavity size leads to an increase of the M–N(sp^3) distances at which the folded conformer(s) become the most stable form: 1.90, 2.14 and 2.18 Å for 12-, 13- and 14-membered macrocycles, respectively.

Introduction

In the last few years we have investigated a series of tetraazamacrocycles containing a pyridine ring in their backbone together with their N-derivatives. The protonation reactions of these compounds as well as their co-ordination behaviour with di- and tri-valent metal ions have been studied.[1–8]

The structures of several metal transition complexes were investigated by X-ray diffraction[2,5–8] and molecular mechanics (MM) calculations were carried out[2,6] in order to evaluate the steric flexibility of these macrocycles in encapsulating metal ions with different stereo-electronic properties and different sizes. These calculations allowed us to understand the role of related structural features, especially the importance of the fit between the metal ion (guest) size and the cavity size provided by the macrocyclic framework (host) on the selectivity of guests. However, most of the work was concentrated on a study of the 14-membered derivative L^3 (3,7,11,17-tetraazabicyclo-[11.3.1]heptadeca-1(17),13,15-triene) and its *N*-methyl carboxylates,[3–6] *N*-methylpyridines[7] and *N*-methylferrocenyl.[8]

In this study we present the crystal structure determinations of a copper(II) complex of the 12-membered macrocycle L^1, and of a copper(II) and a nickel(II) complex of the 13-membered macrocycle L^2. A study of both these macrocycles and their first row transition metal complexes in solution has been undertaken previously,[1] but at that time no crystal structure had been determined. The structures now determined offer the possibility of investigating the effect of cavity size, by the successive increase of the macrocyclic framework with one CH_2 unit, on the co-ordination behaviour of this series of macrocycles, L^1, L^2 and L^3, as well as their N-alkyl derivatives. MM

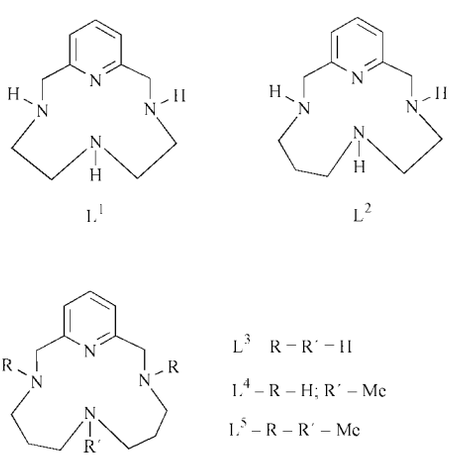

Scheme 1

 DOI: 10.1039/b009773j

calculations were carried out previously for the metal complexes of L^3 (ref. 2), and in this paper we extend them to complexes of the smaller cavity size macrocycles, L^1 and L^2, completing the structural and molecular modelling studies dedicated to this family of macrocycles as hosts for transition metals of the first row of the Periodic Table. With the present study the best-fit sizes for metal ions in 12- to 14-membered tetra-azamacrocycles containing a pyridine ring in the backbone are determined.

Crystallographic and molecular mechanics studies

Crystal structures

The solid state structures of macrocyclic complexes $[CuL^1Br]ClO_4$ **1**, $[CuL^2Br]PF_6$ **2** and $[NiL^2][ClO_4]_2$ **3** were determined by single crystal X-ray diffraction. To the best of our knowledge these crystal structures represent the first X-ray determinations of transition metal complexes of both macrocycles. Indeed, no structures were retrieved for L^2 in a search on the Cambridge Data Base,[9] while only three for the free macrocycle L^1 were found, L^1·HCl (ref. 10), $(H_3L^1)_2(SiF_6)_3·4H_2O$ (ref. 11) and $(H_3L^1)_2GeF_6(NO_3)_4$ (ref. 12).

Selected bond lengths and angles for the three complex cations, listed in Table 1, indicate that the copper atoms in complexes of L^1 and L^2 have co-ordination spheres of the [4 + 1] type while the nickel atom in the complex of L^2 is four-co-ordinate.

The asymmetric unit of complex **1** contains two $[CuL^1Br]^+$ cations and two ClO_4^- anions. One of the anions is disordered over two positions with different statistical occupations (see Experimental section). The molecular dimensions listed in Table 1 for the copper co-ordination sphere clearly show that these two cations have slightly different overall geometries. PLATON[13] diagrams showing the molecular structures of the two independent cations and the atomic labelling scheme adopted are presented in Fig. 1. The four nitrogen donors of L^1 and the bromine form a distorted square pyramidal co-ordination arrangement around the copper centre in molecule **A** (Fig. 1a), while in **B** these donor atoms are intermediate between that geometry and trigonal bipyramidal (Fig. 1b). The root mean square deviation of angles subtended at the metal is only 9.7° between the two structures. In **A** the basal plane is defined by three nitrogen atoms of the macrocycle [N(1), N(4), N(7)] and one bromine leading to angles N(4)–Cu–Br and N(1)–Cu–N(7) of 144.4(2) and 158.8(4)° respectively. The apical position is occupied by the nitrogen N(10) opposite to the pyridine ring. The bond Cu–N(10) is almost perpendicular to the N_3Br basal plane intersecting at an angle of 87.6(3)°. By contrast in **B** the angles centred at the copper atom, N(4)–Cu–N(10), N(4)–Cu–Br and N(10)–Cu–Br, have values of 123.4(3), 126.1(2) and 110.6(3)°, respectively, which suggests a distorted bipyramidal geometric arrangement. The equatorial plane is defined by the nitrogen atoms N(4) and N(10) of the macrocyclic backbone and bromine while the axial positions are occupied by the nitrogen atoms N(1) and N(7), giving rise to an N(1)–Cu–N(7) angle of 152.6(4)°. Furthermore, the vector defined by the atomic positions of the two axial nitrogen donor atoms is nearly perpendicular to the equatorial plane, intersecting at an angle of 89.1(2)°.

The asymmetric unit of complex **2** contains one complex cation, $[CuL^2Br]^+$, and one disordered PF_6^- anion. A PLATON[13] diagram of the complex cation together with the atomic labelling scheme used is shown in Fig. 2. The complex cation also exhibits a distorted square pyramidal environment, but in this case the basal plane is defined by the four nitrogen atoms of the macrocycle with the angles N(4)–Cu–N(10) and N(1)–Cu–N(7) taking values of 143.4(2) and 158.1(2)°, respectively. The axial site is occupied by the bromine atom, which is 2.996(3) Å from the least-squares plane determined by the

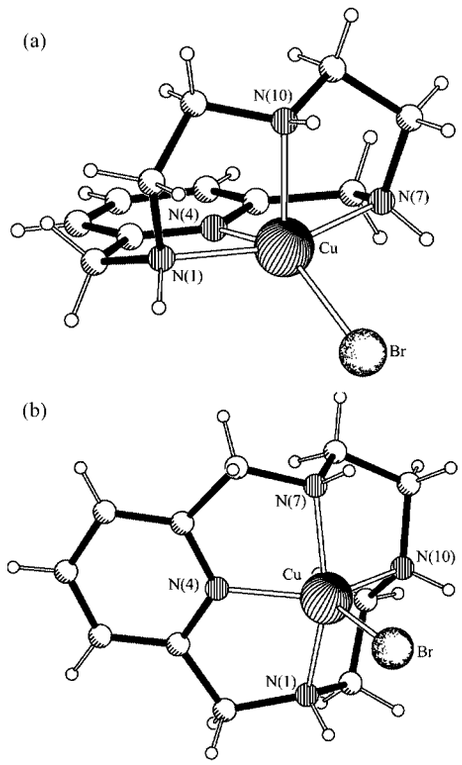

Fig. 1 PLATON diagrams of $[CuL^1Br]^+$ **1** showing the different co-ordination environments of the two independent molecules and the labelling adopted: (a) molecule **A** with a distorted square pyramidal geometry; (b) molecule **B** with distorted bipyramidal geometry. For clarity only the notation for the atoms quoted in the text is included.

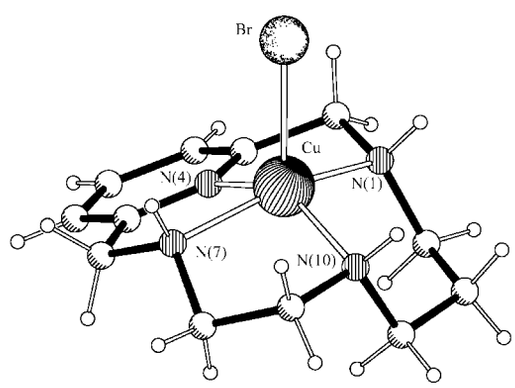

Fig. 2 A PLATON diagram of $[CuL^2Br]^+$ **2** showing the molecular geometry and the labelling scheme adopted. For clarity only the notation for the atoms quoted in the text is included.

atoms N(1), N(4), N(7) and N(10). The copper centre is 0.472(3) Å away from this plane with a Cu–Br distance of 2.499(1) Å. The Cu–Br bond and the N_4 basal co-ordination plane are almost perpendicular intersecting at an angle of 89.1(1)°.

The asymmetric unit of complex **3** comprises one cationic unit, $[NiL^2]^{2+}$, which is disordered such that several atoms occupy two sites with equal probability, and two ClO_4^- anions one of which is also disordered over two sites. A PLATON[13] view of the molecular structure is shown in Fig. 3, ignoring one of the components of the disorder model, and the labelling scheme adopted. The nitrogen N(10) *trans* to the pyridine ring and the bonded carbon atom C(11) are found in two alternative positions, in such a way that in 50% of the cations the ethane chain of the macrocyclic framework is formed by the carbon atoms C(8) and C(9) and the propane chain by C(11), C(12) and C(13), while in the remaining 50% of the cations the reverse situation is observed with the five- and six-membered rings on the opposite sides. Thus the two disordered components are

Table 1 Molecular dimensions of the metal co-ordination sphere(s) of complexes **1**, **2** and **3**

	1, M = Cu(II)		**2**	**3**[a]
	Molecule **A**	Molecule **B**	M = Cu(II)	M = Ni(II)
Bond lengths/Å				
M–N(1)	2.054(9)	2.067(10)	2.027(6)	1.899(4)
M–N(4)	1.965(9)	1.945(8)	1.942(6)	1.805(4)
M–N(7)	2.077(9)	2.026(10)	2.039(5)	1.900(4)
M–N(10)	2.146(9)	2.058(9)	2.003(6)	1.906(9), *1.959(10)*
M–Br	2.384(3)	2.430(3)	2.499(1)	
Bond angles/°				
N(1)–M–N(7)	158.8(4)	152.6(4)	158.1(2)	171.2(2)
N(4)–M–N(10)	102.2(3)	123.4(3)	143.4(2)	167.1(4), *166.3(4)*
N(4)–M–Br	144.4(2)	126.1(2)	112.2(2)	
N(10)–M–Br	113.3(2)	110.6(3)	103.9(2)	
N(4)–M–N(1)	82.5(4)	81.5(3)	81.7(2)	85.0(2)
N(4)–M–N(7)	80.8(4)	80.6(4)	81.7(2)	86.1(2)
N(1)–M–N(10)	86.2(4)	86.3(4)	98.0(3)	102.1(3), *87.6(3)*
N(7)–M–N(10)	84.6(4)	86.3(4)	87.0(3)	86.7(3), *101.0(3)*
N(1)–M–Br	99.8(3)	102.2(3)	99.4(2)	
N(7)–M–Br	101.3(2)	105.1(3)	100.1(2)	

[a] Values in italics correspond to the second component of the disorder model.

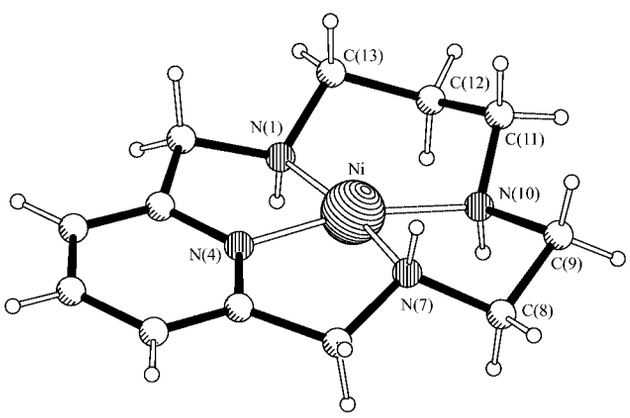

Fig. 3 A PLATON diagram of $[NiL^2]^{2+}$ **3**. Details as in Fig. 2.

pseudo-related by a twofold axis passing through the nitrogen atom N(4) and the nickel centre. The four nitrogen atoms of L^2 form a distorted square planar environment around the metal atom. The disordered model found for the macrocyclic framework leads to two structures with slightly different geometries. In the nickel co-ordination sphere the distance involving the nitrogen *trans* to the pyridine ring exhibits the largest difference between the two structures [Ni–N(10) 1.906(9) *versus* 1.959(10) Å]. However this seems to be more a consequence of the disorder model rather than a significant structural result. In fact, the angles centred at the nickel atom and involving N(10) are very similar for the two components of the disorder. Furthermore the two components display identical macrocyclic conformations. Indeed the fitting of the atomic positions of the sixteen non-hydrogen atoms of the macrocyclic framework of the two components leads to a root mean square deviation of only 0.065 Å.

As would be expected[9] for metal complexes of macrocycles containing a pyridine moiety in the three metal complexes under study the M–N(sp^2) is shorter than the remaining three M–N(sp^3) distances.

Macrocyclic conformations of transition metal complexes

The conformations adopted by the 14-membered macrocycle L^3 as well as its N-derivatives in metal complexes have been described in terms of the positions of the NH hydrogen atoms or N-substituent groups being either above (+) or below (−) the N_4 macrocyclic plane.[2] For a square planar geometry there are therefore three different planar conformers: +++, −+− and −−+. The metal centre is often slightly displaced from the plane determined by the four nitrogen donor atoms. For the 12-membered macrocycle L^1 only these three arrangements are also possible, because both macrocycles have symmetric frameworks. The insertion of one CH_2 group into the backbone of L^1 to give L^2 results in an asymmetric macrocycle and so one extra conformer must be considered. The arrangement −−+ in L^1 leads to two geometric isomers in L^2 depending on whether the N–H + group above the plane belongs to a five- or a six-membered chelating ring. These two conformers are designated in this manuscript by −−+[5] when the N–H + group is common to two five-membered chelating rings and −−+[6] when it is between one six- and one five-membered chelating ring. In square pyramidal geometries the number of possible conformations for the three macrocycles is at least twice that of the square planar depending on the orientation of the N–H groups relative to the fifth ligand, which may also occupy an equatorial or an axial position. The labels e and a are used to indicate precisely the equatorial or axial position of the monodentate ligand in the metal co-ordination sphere. All possible conformers for L^1 and L^2 are defined in Figs. 4 and 5.

Following this nomenclature the macrocycle L^1, in the complexes **1A** and **1B** determined by single crystal X-ray diffraction, displays a folded conformation of the type +++e, while L^2 adopts in **2** the planar conformation +++a. In both complexes the positions of the N–H groups are designated by + because the hydrogen atoms and the bromine are located on the same side of the N_4 plane (see Figs. 1 and 2). Both components of disorder in complex **3** give rise to a −−+[5] conformation.

As mentioned before, there are no experimental X-ray data available in the CSD[9] for metal complexes of L^1 and L^2. By contrast some structures of the first row transition metal complexes of the 14-membered macrocycle L^3 and their N-methyl derivatives, L^4 and L^5, were found. These complexes are listed in Table 2 together with their CSD refcodes and relevant structural parameters for characterisation of their co-ordination sphere together with data for the compounds under study. The comparison of the structural data listed for the 14-membered macrocycles together with those of the 12- and 13-membered macrocycles available in this work offers the possibility of evaluating the effect of the macrocyclic cavity size on the

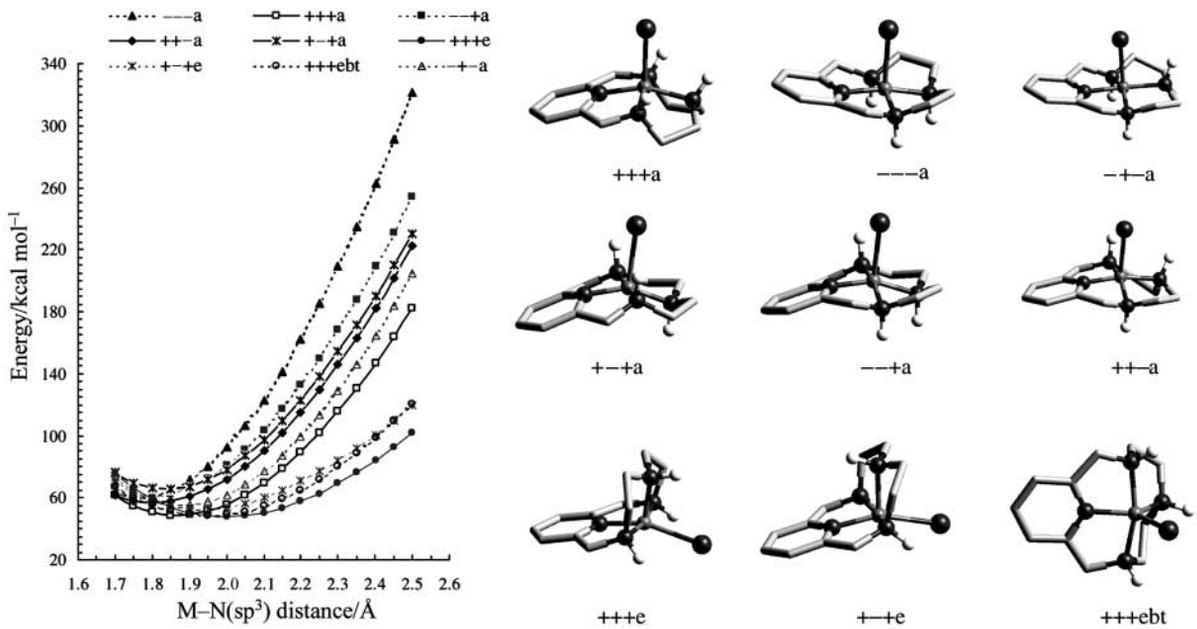

Fig. 4 Steric energy *versus* M–N(sp^3) distance for trigonal bipyramidal and square pyramidal complexes [ML^{1}Br] with sketches of all relevant conformations. The M–N(sp^2) distances are changed concomitantly with the M–N(sp^3) distance, the difference between them being 0.1 Å along the range of M–N distances taken into account in MM calculations.

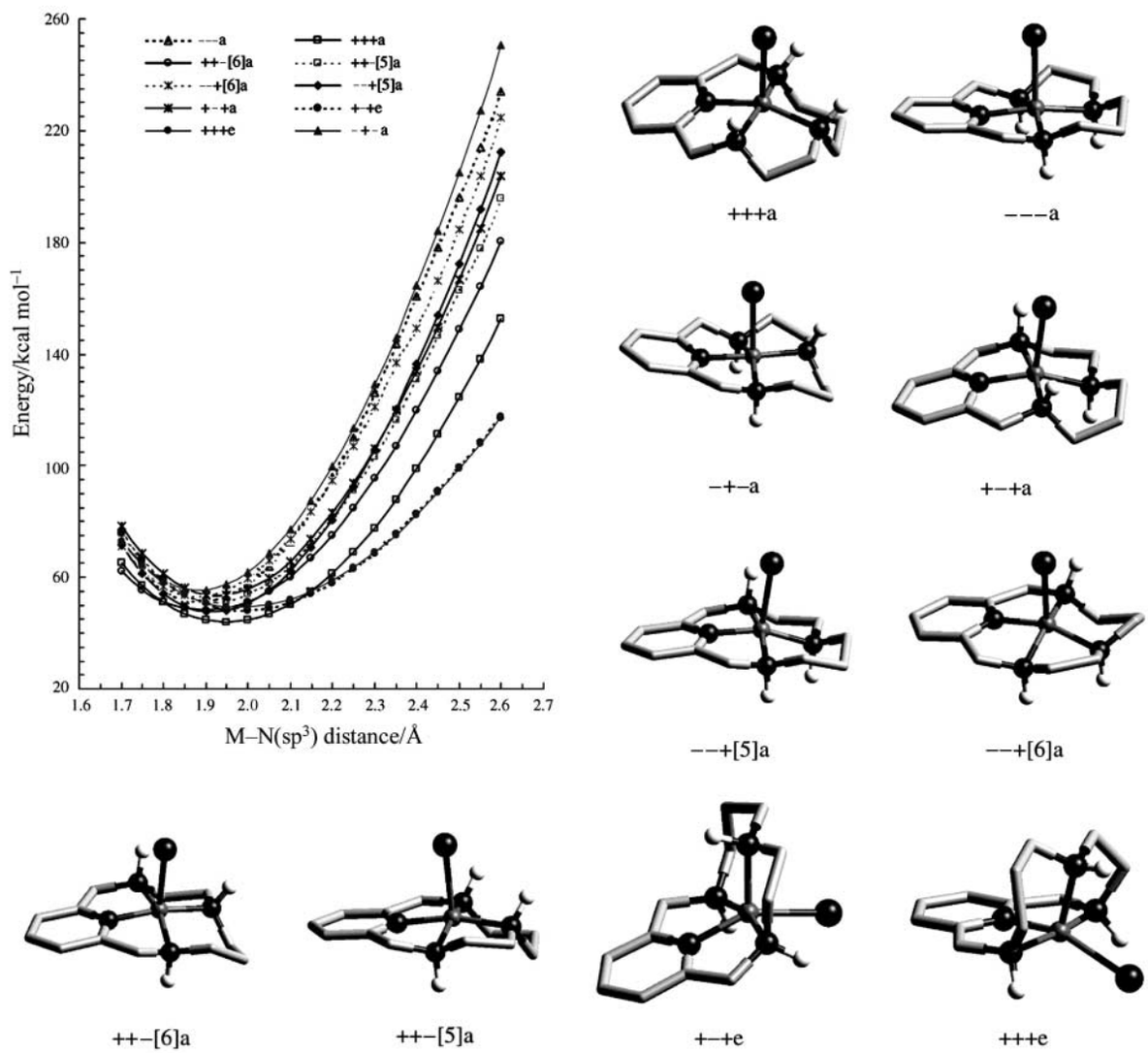

Fig. 5 Steric energy *versus* M–N(sp^3) distance for square pyramidal complexes [ML^{2}Br] with sketches of all relevant conformations. Details as given in Fig. 4.

Table 2 Relevant structural parameters for characterisation of the co-ordination mode of tetra-aza macrocycles containing a pyridine ring[a]

Complex	M–N(sp²)/Å	⟨M–N(sp³)⟩/Å	Deviations (Å) of donor atoms from the mean least-squares equatorial plane					*D*/Å	*Ω*/°	Conformation	Refcode
			N(1)	N(4)	N(7)	N(10)	X				
$[CuL^1Br]^+$											This work
1A	1.965(9)	2.092(9)	0.374	−0.485	0.372		−0.261 (Br)	0.272	60.0	+++e	
1B	1.945(8)	2.050(10)		0.000		0.000	0.000 (Br)		30.4	+++e	
$[CuL^2Br]^+$ **2**	1.942(6)	2.023(6)	0.133	−0.156	0.145	−0.122		0.472	17.3	+++a	This work
$[CuL^4(NO_3)]^+$ **4**	1.934(2)	2.027(2)	−0.090	0.115	−0.100	0.084		0.239	12.0	−−−a	NUTJAN
$[NiL^5(H_2O)]^{2+}$ **6**	1.974(4)	2.085(4)	0.040	−0.046	0.040		−0.034 (O)	0.353	77.5	+−+e	DOCVIA
$[NiL^5(dmso)]^{2+}$ **7**	1.97(3)	2.10(3)	0.029	−0.033	0.029		−0.025 (O)	0.361	101.9	+−+e	FEJMUC
$[NiL^5Cl]^+$ **8**	1.976(3)	2.088(5)	0.055	−0.068	0.056		−0.043 (Cl)	0.375	77.2	+−+e	FEJNAJ
$[NiL^2]^{2+}$ **3**	1.805(4)	1.902(4)	0.075	−0.088	0.084	−0.071		0.092	10.0	−−+[5]	This work
	1.805(4)	*1.919(6)*	*0.091*	*−0.096*	*0.080*	*−0.076*		*0.104*	*10.7*	−−+[5]	
$[CuL^3]^{2+}$ **9**	1.904(8)	2.015(8)	−0.143	0.168	−0.144	0.120		0.133	17.6	−−−	REDYEE
$[NiL^4]^{2+}$ **5**	1.848(4)	1.944(4)	−0.045	0.051	−0.045	0.039		0.114	5.6	−−−a	REDYII
$[NiL^5]^{2+}$ **10**	1.866(3)	1.987(4)	−0.115	0.134	−0.115	0.096		0.090	14.2	−−−	DOCVEW
$[NiL^5]^{2+}$ **11**	1.82(2)	1.98(2)	−0.030	0.035	−0.029	0.024		0.006	3.8	++−	FEJMOW

[a] The donor atoms are labelled using the atomic notation presented in Figs. 1, 2 and 3 for the studied complexes. L^4, L^5 are N-methyl derivatives of the 14-membered tetra-aza macrocycle L^3. *D* represents the distance from the metal centre to the mean least-squares basal plane, *Ω* is the macrocyclic folding angle defined in the text. The italic values refer to the second component of the disorder. For simplicity the complex cations and the corresponding neutral species are labelled similarly.

structural preferences of these ligands and on the molecular dimensions of the metal co-ordination spheres. Furthermore establishing the flexibility of these ligands allows us also to evaluate their capability to encapsulate metal ions with different sizes and stereo-electronic preferences.

The deviations from the least-square planes defined through the equatorial co-ordination planes show that the most pronounced tetrahedral distortion is exhibited by complex **1A**, where the 12-membered macrocycle L^1 encapsulates the copper centre in a folded square pyramidal geometric arrangement. The folding of the macrocyclic ring along the axis defined by the nitrogen atoms neighbouring to the pyridine ring can be measured by the folding angle (Ω), which corresponds to the dihedral angle between the planes [N(1),N(4),N(7)] and [N(1),N(10),N(7)] (see Figs. 1, 2 and 3) in the crystal structures reported here. The complex **1A** exhibits a Ω angle of 60.0(4)° which is significantly reduced to 30.4(1)° in **1B**, where the nitrogen *trans* to pyridine ring [N(10)] occupies an equatorial site position distorted towards a trigonal bipyramidal arrangement. A more pronounced folding is reported for the macrocycle L^5 in the square pyramidal complexes $[NiL^5(H_2O)]^{2+}$ **6** (77.5°), $[NiL^5(dmso)]^{2+}$ **7** (101.9°) and $[NiL^5Cl]^+$ **8** (77.2°), where the nitrogen *trans* to the pyridine ring and the monodentate ligand are located respectively in the apical and basal positions as observed in complex **1A** (see Table 2).

When the four nitrogen donor atoms of the macrocycle ring form a square planar arrangement around the metal centre small values for Ω are expected. Thus in the 13-membered macrocyclic complexes $[CuL^2Br]^+$ **2** and $[NiL^2]^{2+}$ **3** the Ω angle takes values of 17.3 and 10.3° (average), respectively. Comparable Ω angles were found for complexes of the 14-membered macrocycle L^3 and its N-methyl derivatives (L^4 and L^5) in the planar conformers $[CuL^3]^{2+}$ **9** (17.6°), $[NiL^5]^{2+}$ **10** (14.2°) and $[CuL^4(NO_3)]^+$ **4** (12.0°), the last one exhibiting a square pyramidal geometry with the NO_3^- in the axial position as a monodentate ligand. Therefore in all these complexes the N_4 co-ordination plane has a comparable distortion. The square planar complexes $[NiL^4]^{2+}$ **5** and $[NiL^5]^{2+}$ **11** display even smaller Ω angles of 5.6 and 3.8° respectively, and slightly smaller tetrahedral distortions were found.

Additionally in five-co-ordinate complexes such as **2** or **4** the copper centre is displaced from the N_4 co-ordination plane towards the apical ligand by 0.472 and 0.239 Å, respectively. On the other hand, in the square planar complexes, **3** and **10**, the nickel centre is displaced from the equatorial N_4 plane by only 0.098 (average) and 0.090 Å respectively, and in **11** the nickel atom is coplanar within experimental error with a displacement of 0.006 Å. The latter results clearly indicate that the nickel ion fits reasonably well in the planar cavity provided either by the 13- or the 14-membered macrocycles. A small deviation of 0.133 Å of the copper centre from the N_4 co-ordination plane was found in complex **9**.

So the X-ray structural data of 12-, 13-, and 14-membered macrocyclic complexes collected in Table 2 clearly show that for macrocycles of small cavity sizes, such as L^1, the incorporation of the metal centre into the cavity is only possible because the macrocycle has enough flexibility to fold and distort. In fact, as mentioned above, the two independent cations of **1** exhibit two different distorted five-co-ordination environments, in which the copper centre is encapsulated by the macrocycle in a folded conformation +++e. By contrast in complexes **2** and **3** the 13-membered macrocycle L^2 adopts a planar arrangement around the metal centre. These results indicate that L^2 is able to achieve a planar conformation with a large enough cavity to accommodate metal ions such as Ni^{2+} and Cu^{2+}. Consequently, planar conformers for the complexes of the 14-membered macrocycle L^3 and its derivatives will be expected and indeed are observed (see Table 2). In the square planar complexes of L^2, L^3 and L^5 the metal centres are only slightly displaced from the N_4 macrocyclic plane indicating that ions such as Ni^{2+} or Cu^{2+} fit comfortably into the larger cavities provided by these 13- and 14-membered macrocycles. The macrocycle L^2 in **3** shows a −−+[5] conformation while L^5 in the nickel complexes **11** and **10** adopts the ++− and −−− conformations respectively, the latter being also adopted by L^3 in **9**. Furthermore, as expected in planar conformers with square pyramidal geometry, such as are found in complexes **2** and **4**, the copper centre is displaced from the plane in the direction of the apical ligand, but with larger deviations in **2** (0.472 Å) than in **4** (0.239 Å), no doubt because the cavity size of the 13-membered macrocycle L^2 is smaller than that of the 14-membered macrocycle L^4.

It is also interesting that the five-co-ordinate nickel complexes of L^5 in Table 2 exhibit a co-ordination environment of the type found in **1**, but the folded conformation adopted by the macrocycle is +−+e rather than +++e.

Molecular mechanics calculations

In previous work we reported molecular mechanics calculations for the 14-membered macrocycle L^3 and its N-methyl derivatives in four- and five-co-ordination environments.[2] Here we extend these calculations to the 12- and 13-membered macrocycles L^1 and L^2 respectively, but only considering the co-ordination number of 5. In both studies the MM calculations were carried out with the universal force field[14] using a similar molecular modelling methodology as before (see Experimental section). Therefore the results obtained can directly be compared, and consequently the effect of the dimensions of the macrocycle, by adding CH_2 units, along the series L^1, L^2 and L^3 can unambiguously be determined.

Results for the five-co-ordinate complexes of $[ML^1Br]$ are shown in Fig. 4 and those of $[ML^2Br]$ in Fig. 5. The figures include plots of the changes of steric energy *versus* the M–N(sp^3) distances, as well as 3-D sketches of all the conformers taken into account in the molecular mechanics calculations. All curves plotted have broad profiles over the wide ranges of M–N distances studied indicating that the macrocyclic frameworks of L^1 and L^2 have enough steric flexibility to accommodate metal ions with different sizes.

For L^1 in the square pyramidal arrangement we have considered six different conformers containing the monodentate ligand in an apical position, +++a, −−−a, −+−a, +−+a, −−+a, ++−a, and two conformers having the monodentate ligand in an equatorial position, +++e and +−+e. For planar conformers the sign (+ or −) characterises the position of the corresponding N–H group relative to the apical ligand. In addition the +++e conformer is also evaluated in a constrained trigonal bipyramidal (bt) geometric arrangement, because a distorted form of this type of geometry was observed for one of the two independent molecules of the crystal structure of **1**, +++ebt (see above). Other possible geometric arrangements resulting from different stereochemistries of the three sp^3 nitrogen atoms of L^1 are not sterically allowed. From Fig. 4 it can be observed that the curves of steric energy as a function of the M–N(sp^3) distance, calculated for all the conformers, display broad minima exhibiting small energy differences up to 1.90 Å, but in this range the +++a conformer has the lowest energy. Between 1.90 and 2.00 Å the +++e and +++ebt conformers share the lowest energy, and finally the +++e conformation is the preferred one for longer M–N(sp^3) distances. The stabilisation of both +++e and +++ebt conformers in the range 1.90–2.00 Å is entirely consistent with the crystal structure determination of complex **1**. The two independent molecules $[CuL^1Br]^+$ **1A** and **1B** have distorted square pyramidal geometries with average Cu–N(sp^3) distances of 2.09 and 2.05 Å, respectively. The corresponding theoretical curves for the ideal geometries at these distances are barely distinguishable, the energy difference being only about 4.0 kcal mol^{-1} at 2.09 Å. These energies can be compared since the calculations were carried out in the gas phase and the distortions were modelled

using a force field which included ideal angles subtended at the metal centre (see Experimental section).

The asymmetry of the 13-membered macrocycle L^2 required the consideration of a considerable number of independent conformations, as shown in Fig. 5. As explained above, the $++-$a and $--+$a forms of the symmetric macrocycle L^1 give rise to four different conformers in the case of L^2 which are called $++-$[5]a, $++-$[6]a, $--+$[5]a and $--+$[6]a. The remaining four conformers which contain the fifth ligand in the apical position are $---$a, $+++$a, $-+-$a and $+-+$a. Similarly to what has been described for L^1 there are also two folded conformers $+++$e and $+-+$e. The $++-$[6]a conformer is preferred for short M–N(sp^3) distances up to 1.80 Å, the $+++$a conformer between 1.80 and 2.14 Å while both $+++$e and $+-+$e forms show the lowest steric energy for longer M–N(sp^3) distances. Again the theoretical and experimental results are in agreement since the $+++$a form is found in the crystal structure of $[CuL^2Br]^+$ **2** and the average M–N(sp^3) distance of 2.02 Å is within the broad minimum of the corresponding curve.

The MM calculations carried out for L^3, previously reported[2] using the species $[ML^3Cl]$, have shown that the most stable conformers at short M–N distances all have the chloride in the apical position. Thus the $+++$a conformer is the most stable for M–N distances up to 1.90 Å, followed by the $--+$a conformer between 1.90 and 2.05 Å and the $---$a conformer between 2.05 and 2.18 Å. Finally for longer distances the $+-+$e conformer becomes the most stable. On the other hand, replacement of the three N-hydrogen atoms of L^3 by N-methyl groups to give L^5 leads to stabilisation of the folded equatorial conformer ($+--$e) in the complete range of M–L distances studied, although its energy is barely distinguishable from that of the $---$a conformer near their minima between 1.95 and 2.25 Å. These results are entirely consistent with crystal structures of metal complexes of L^3–L^5 quoted in Table 2, in that complexes of L^4 display the $---$a conformation while those of L^5 exhibit the $+-+$e conformer.

Conclusion

The molecular mechanics and structural results presented for the 12- to 14-membered macrocycles L^1–L^5 clearly show that the macrocycles of smaller cavity size prefer the planar conformation $+++$a to accommodate small metal ions, corresponding to ideal M–N(sp^3) distances of up to 1.90 Å. However for longer distances the 12-membered framework has enough flexibility to fold and the $+++$e conformation clearly becomes the preferred one. With the larger dimensions found for the 14-membered rings, L^3–L^5, the $+++$a is also the most stable conformation for M–N(sp^3) distances up to 1.90 Å, however the folded $+-+$e conformation only becomes the most stable for distances longer than 2.18 Å. Between these two values, the two conformations having a monodentate apical ligand are preferred ($--+$a between 1.90 and 2.05 Å, and $---$a between 2.05 and 2.18 Å). The 13-membered ring exhibits intermediate behaviour adopting folded conformations for distances longer than 2.14 Å, $+++$e and $+-+$e, respectively, the former being found for the 12-membered and the latter for the 14-membered macrocycle. Thus these two conformations have the same probability of occurring in complexes of larger metal ions with L^2. It is also apparent that increasing the macrocyclic cavity size results in a clear and concomitant increase of the M–N(sp^3) distances at which the folded conformer(s) become the most stable form: *e.g.* 1.90, 2.14 and 2.18 Å for the 12-, 13- and 14-membered macrocycles, respectively.

Another striking fact which emerges from these molecular mechanics studies is that the $---$a conformer only appears among the most stable conformations for the 14-membered macrocycle. In other words, this conformation, in which the metal ion and all hydrogens bound to nitrogen atoms are on opposite sides of the donor plane, is unlikely to be observed for the 12- and 13-membered macrocycles.

To aid understanding of this last observation we present in Fig. 6 the ball and stick representations of $+++$a and $---$a MM minimised conformers for the 12-, 13-, and 14-membered macrocycles (L^1, L^2 and L^3) as well as Newman projections for the ethane and propane chains. The optimised structures correspond to the conformations with lowest strain energy values found for the large range M–N(sp^3) and M–N(sp^2) distances studied, see Figs. 4 and 5. The Newman projections for the $+++$a conformer of the 12-membered macrocycle L^1 show that the two ethane chains of this ligand adopt a staggered arrangement, while in the $---$a conformer both chains display a nearly eclipsed arrangement which is obviously sterically less stable. Furthermore, in the case of the $+++$a conformer the metal ion is clearly above the N_4 donor atoms plane and as the nitrogen lone pairs are directed towards the metal ion, consequently the N–H groups are directed to the external side of the macrocyclic ring. In this form the apical ligand and the ethane bridges are on opposite sides giving additional steric stability to this conformation. By contrast in the $---$a conformer the ethane chains and the apical ligand are on the same side of the N_4 macrocyclic co-ordination plane. A similar situation occurs with complexes of the 12-membered tetra-aza macrocycle cyclen (1,4,7,10-tetra-azacyclododecane)[9] and is explained by Hancock *et al.* using a similar structural model.[15] In the case of the 14-membered macrocycle, represented in Fig. 6(c), the three CH_2 groups of the two propane chains show sterically stable staggered arrangements in both conformers, $+++$a and $---$a. However in the latter conformer additional stability is provided by the relative position of the hydrogens bound to the nitrogen donor atoms and the apical ligand, which are on opposite sides of the N_4 donor atoms of the co-ordination plane. As expected, the 13-membered macrocycle displays an intermediate situation as shown in Fig. 6(b). In other words, in the $+++$a conformer the ethane chains of the five- and six-membered chelate rings adopt staggered arrangements, while in the $---$a conformer the ethane chain of the five-membered chelate ring exhibits an almost eclipsed arrangement as found in the 12-membered macrocycle, while the ethane chains of the six-membered chelate ring have staggered arrangements comparable to those reported for the 14-membered macrocycle.

These molecular calculations were necessarily carried out in the gas phase. However because the macrocycles encapsulate the metal atoms it seems likely that similar structures would be found in solution. With predominantly monodentate or bidentate ligands this is less likely and it might be necessary to include solvent either implicitly or explicitly in the calculations.

It is difficult to cater exactly in a molecular mechanics force field for electronic effects and resulting structural distortions but our calculations are sufficiently quantitative to be consistent with experimental results from crystal structure determinations.

Experimental

Reagents

The macrocycles L^1 and L^2 were synthesized by previously reported procedures.[1] All the chemicals were of reagent grade and used as supplied without further purification. **CAUTION:** although no problems were found in this work, perchlorates in the presence of organic matter are potentially explosive and should be prepared in small quantities.

Syntheses

$[CuL^1Br]ClO_4$ 1. $Cu(ClO_4)_2 \cdot 6H_2O$ (0.1 mmol, 0.037 g) was added to a stirred solution of $L^1 \cdot 3HBr$ (0.1 mmol, 0.0446 g) dissolved in the minimum volume of water (≈2 cm^3) and the pH

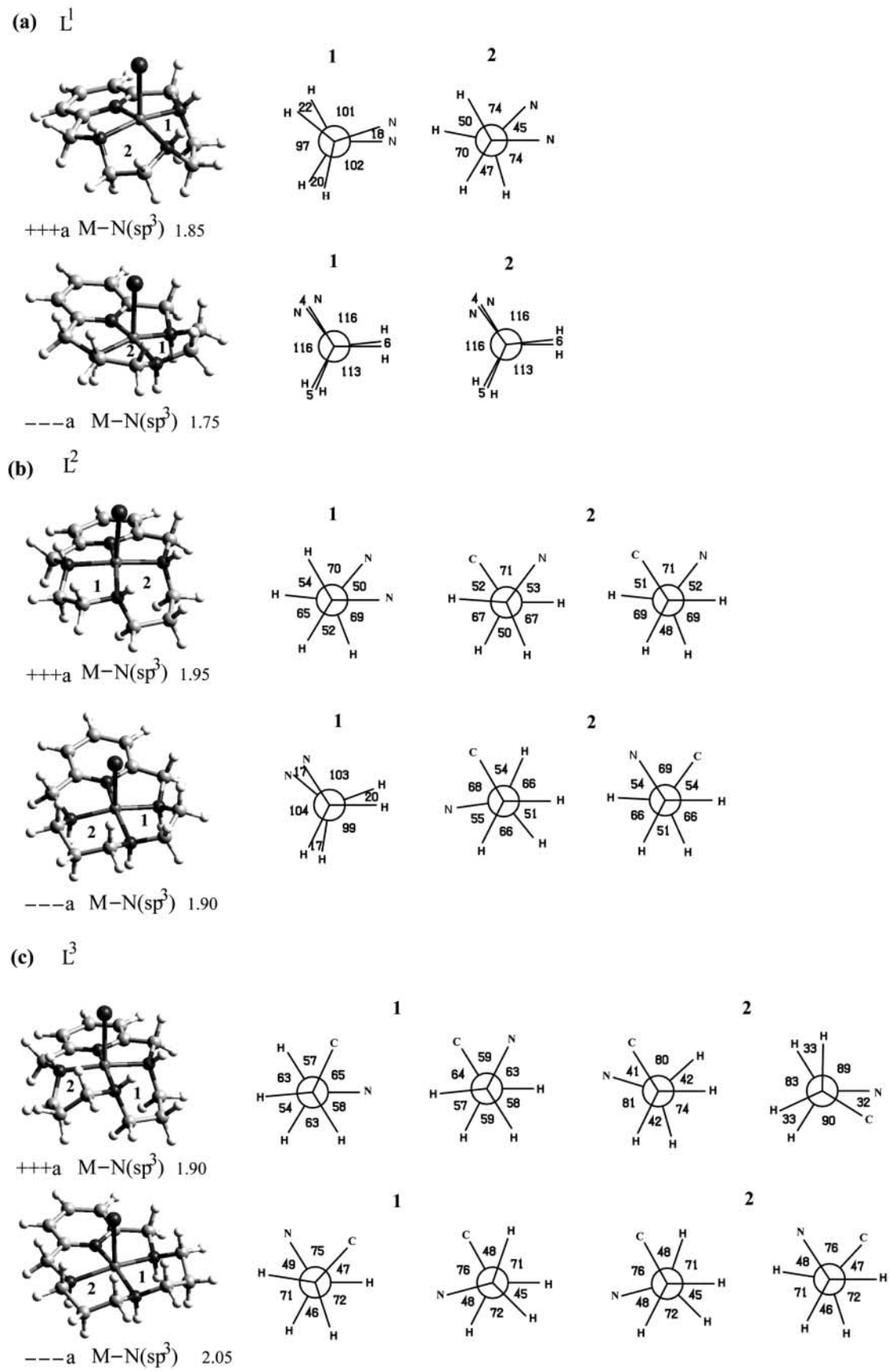

Fig. 6 Ball and stick representations of +++a and ---a MM minimised conformers for the L^1 (a), L^2 (b), and L^3 (c) macrocycles and their Newman projections for the ethane and propane chains including the torsion angles (°) around the C–C bonds. The Newman projections are listed successively starting at ring 1 (at the nitrogen atom contiguous to the pyridine moiety) and finishing at ring 2. The distances (Å) for energy minima are given.

increased to 5.2 by addition of KOH. The mixture was stirred for 2 h and then concentrated to dryness. The residue was taken up in methanol, the precipitate formed filtered off and the filtrate again concentrated to dryness and the residue dissolved in a mixture of ethanol and acetonitrile. Blue crystals were formed in six weeks by slow evaporation of the solvent. Yield: ≈90%.

Table 3 Room temperature crystal data and the pertinent refinement parameters for complexes **1**, **2** and **3**

	1	**2**	**3**
Empirical formula	$C_{11}H_{18}BrClCuN_4O_4$	$C_{12}H_{20}BrCuF_6N_4P$	$C_{12}H_{20}Cl_2N_4NiO_8$
M	449.19	508.74	477.93
Crystal system	Orthorhombic	Triclinic	Triclinic
Space group	$P2_1/a$	$P\bar{1}$	$P\bar{1}$
a/Å	7.950(11)	8.559(3)	8.162(2)
b/Å	22.307(27)	9.592(3)	8.874(2)
c/Å	18.298(23)	11.803(3)	13.989(2)
α/°		77.69(2)	91.36(3)
β/°	[a]	75.19(2)	104.48(2)
γ/°		88.56(2)	113.52(2)
V/Å^3	3245(7)	914.9(5)	890.8(4)
Z	8	2	2
μ/mm^{-1}	3.995	3.526	1.767
Reflections measured	9223	6907	3742
Unique reflections	5383 (R_{int} = 0.0448)	4411 (R_{int} = 0.1249)	3500 (R_{int} = 0.0108)
R and R_w [$I > 2\sigma(I)$]	0.0703, 0.1862	0.0731, 0.1745	0.0690, 0.1826
(all unique data)	0.1203, 0.2129	0.1070, 0.2043	0.0772, 0.1943

[a] No significant deviation from 90.0° could be observed in this twinned crystal.

Found: C, 29.1; H, 4.1; N, 12.1%. Calc. for $C_{11}H_{18}BrClCuN_4O_4$: C, 29.4; H, 4.0; N, 12.5%.

[CuL^{2}Br]PF$_6$ 2. A mixture of $CuCl_2 \cdot 2H_2O$ (0.05 mmol, 0.00852 g) and L$^2 \cdot$3HBr (0.05 mmol, 0.023 g) in water (≈2 cm^3) at pH 6.3 (by addition of 3 mol dm^{-3} KOH) was stirred for 2 h and then $TlPF_6$ (0.05 mmol, 0.175 g) added. A white precipitate was formed and filtered off. The solution was concentrated to dryness and the residue taken up in methanol. The precipitate formed was filtered off and the filtrate again concentrated. Blue crystals suitable for X-ray determination were formed in a few days by slow evaporation of the remaining solvent. Yield: ≈90%. Found: C, 28.3; H, 3.7; N, 10.9%. Calc. for $C_{12}H_{20}BrCuF_6N_4P$: C, 28.3; H, 4.0; N, 11.0%.

[NiL^2][ClO$_4$]$_2$ 3. $Ni(ClO_4)_2 \cdot 6H_2O$ (0.492 mmol, 0.180 g) was added to a stirred solution of L$^2 \cdot$3HBr (0.05 mmol, 0.023 g) dissolved in the minimum volume of water (≈2 cm^3) and the pH increased to ≈8 by addition of 3 mol dm^{-3} KOH. The mixture was refluxed for 2 h and then concentrated to dryness. The residue was taken up in a mixture of methanol and acetone. Orange-yellow crystals were formed in a few days by slow evaporation of the solvent at room temperature. Yield: ≈94%. Found: C, 29.2; H, 4.2; N, 11.5%. Calc. for $C_{12}H_{20}Cl_2N_4NiO_8 \cdot H_2O$: C, 29.1; H, 4.5; N, 11.3%.

Crystallography

In Table 3 the crystallographic data are summarised together with data collection and the refinement details for complexes [CuL^{1}Br]ClO$_4$ **1**, [CuL^{2}Br]PF$_6$ **2** and [NiL^2][ClO$_4$]$_2$ **3**.

Crystal data for complex **1** were collected at Reading University using a MAR research image plate system equipped with graphite-monochromated Mo-Kα radiation (λ = 0.71073 Å). Data analysis was performed with the XDS program.[16] Intensities were corrected empirically for absorption effects with the DIFABS program, using a version modified for the image plate system.[17] Crystal data for complexes **2** and **3** were measured at the Instituto Superior Técnico on a CAD4 diffractometer with graphite-monochromated Mo-Kα radiation (λ = 0.71069 Å) by ω–2θ scan mode. Unit cell dimensions for both complexes were obtained by least-squares refinement of the setting angles of 25 reflections with θ between 18 and 25°. Data were corrected for Lorentz, polarisation and linear decay (no decay was observed) as well as empirically for absorption, using the MOLEN software.[18]

The structures of the three complexes were solved by a combination of direct methods and Fourier difference syntheses. The crystal of **1** appeared to be orthorhombic but successful refinement was eventually obtained in monoclinic space group $P2_1/a$ assuming a twinned crystal. The structure refinement was performed using the instruction TWIN 1 0 0 0 0 −1 0 0 −1 2 together with the BASF parameter which refined to 0.23(1). The structure of complex **3** was solved in both space groups of the triclinic system. Refinement in $P1$, with two independent molecules of **3**, was unstable and yielded two structures with some chemically unreasonable dimensions. Alternatively in $P\bar{1}$ two alternative positions for the nitrogen atom *trans* to the pyridine ring [N(10)] and for other atoms were found from Fourier difference maps. Structure refinement was carried out successfully with the disordered model described above.

In complexes **1** and **3** one of the two independent ClO_4^- anions in the asymmetric unit was disordered. In both cases two sets of tetrahedral oxygen atoms were found from the Fourier difference maps and refined with occupancy factors x and $1 - x$; x refined to 0.40(2) for **1** and 0.48(1) for **3**. In the unit cell of complex **2** the PF_6^- anions are disordered over two positions. Two sets of octahedral fluorine atoms sites were refined with occupancy factors x and $1 - x$, x being refined to 0.40(2). The disordered fluorine and oxygen atoms were refined using isotropic thermal parameters the remaining non-H atoms with anisotropic thermal parameters. All hydrogen atoms were inserted in idealised positions and allowed to refine, riding on the parent C (N) atom with an isotropic thermal parameter equal to 1.2 times those of the atom to which they were bonded. The structures were refined by full-matrix least squares against F^2 until the desired convergence was achieved.

The final Fourier difference synthesis revealed residual electron densities of 1.480, −1.247 e Å^{-3} for **2** and 1.491, −0.952 e Å^{-3} for **3**. In both cases the highest positive peaks are near oxygen or fluorine atoms of disordered anions. For complex **1** the residual electron density, ranging between 1.193 and −1.269 e Å^{-3}, was within the expected values. All calculations to solve and refine the structures were carried out with SHELXS and SHELXL from the SHELX 97 package.[19] Molecular and crystal packing diagrams were drawn with PLATON graphical software.[13]

CCDC reference numbers 154180–154182.

See http://www.rsc.org/suppdata/dt/b0/b009773j/ for crystallographic data in CIF or other electronic format.

Molecular mechanics calculations

Molecular mechanics calculations were carried out using the Universal Force Field[14] within the CERIUS 2 software.[20] Default parameters were used apart from the terms involving the metal centre. The angle bending terms at the metal centre for square pyramidal and bipyramidal geometries were treated

individually using a cosine Fourier expansion term in the following manner. For square pyramidal the L_{ax}–M–L_{eq} angles were restrained to 100° while L_{eq}–M–L_{eq} were restrained to 100 or 160°. These bending angle values allow one indirectly to simulate the position of the metal centre out of the basal co-ordination plane. This geometric feature, typical of this geometry, is not available in the CERIUS 2 software but can be imposed *via* the restrain tool. For bipyramidal geometry the angles L_{ax}–M–L_{ax}, L_{eq}–M–L_{eq} and L_{ax}–M–L_{eq} were restrained to 160, 120 and 100°, respectively. For both geometries force constants of 100 kcal mol^{-1} rad^{-2} were used for all angles restrained. M denotes the atom type Cu^{2+} while L_{ax} and L_{eq} represent the atoms N_R, N_3, N_31 or Br respectively. The atom N_31 has the same universal force field properties as those of N_3 and it was created to allow individual assignment of bending angle terms.

The strain energies for different conformers were calculated using a procedure similar to that described before.[2] All four M–N distances were fixed using large force constants of 7000 kcal mol^{-1} $Å^{-2}$ for the stretching terms. A difference of 0.1 Å between M–N(sp^3) and M–N(sp^2) distances was taken into account in all MM calculations since this is observed in most of the crystal structures of transition metal complexes of macrocycles containing pyridine moieties. Then the energy profiles of the conformers relative to M–N distances were obtained by changing concomitantly the M–N(sp^3) and M–N(sp^2) distances successively at 0.05 Å intervals over the range 1.7 to 2.5 Å. Partial charges were not included because they were difficult to calculate accurately and only have marginal impact on relative strain energies in metal complexes.

The starting coordinates for geometric isomers were obtained from the X-ray determinations or alternatively by manipulation of the coordinates of metal complexes where the macrocyclic ligand is co-ordinated to the metal centre in a geometric arrangement similar to the present ones.

Acknowledgements

The authors acknowledge the financial support of FCT and PRAXIS XXI (Project no. PRAXIS/2/2.1/QUI/17/94). We thank the EPSRC (UK) and the University of Reading for funds for the Image Plate System and Mr A. W. Johans for his assistance with the crystallography.

References

1 J. Costa and R. Delgado, *Inorg. Chem.*, 1993, **32**, 5257.
2 V. Félix, M. J. Calhorda, J. Costa, R. Delgado, C. Brito, M. T. Duarte, T. Arcos and M. G. B. Drew, *J. Chem. Soc.*, *Dalton Trans.*, 1996, 4543.
3 R. Delgado, S. Quintino, M. Teixeira and A. Zhang, *J. Chem. Soc.*, *Dalton Trans.*, 1997, 55.
4 J. Costa, R. Delgado, M. C. Figueira, R. T. Henriques and M. Teixeira, *J. Chem. Soc.*, *Dalton Trans.*, 1997, 65.
5 J. Costa, R. Delgado, M. G. B. Drew and V. Félix, *J. Chem. Soc.*, *Dalton Trans.*, 1998, 1063.
6 J. Costa, R. Delgado, M. G. B. Drew, V. Félix, R. T. Henriques and J. C. Waerenborgh, *J. Chem. Soc.*, *Dalton Trans.*, 1999, 3253.
7 J. Costa, R. Delgado, M. G. B. Drew and V. Félix, *J. Chem. Soc.*, *Dalton Trans.*, 1999, 4331.
8 J. Costa, R. Delgado, M. G. B. Drew, V. Félix and A. Saint-Maurice, *J. Chem. Soc.*, *Dalton Trans.*, 2000, 1907.
9 F. H. Allen, J. E. Davies, J. J. Galloy, O. Johnson, O. Kennard, C. F. Macrae, E. M. Mitchell, G. F. Mitchel, J. M. Smith and D. G. Watson, *J. Chem. Inf. Comput. Sci.*, 1991, **31**, 187.
10 W. D. Kim, D. C. Hrncir, G. E. Kiefer and A. D. Sherry, *Inorg. Chem.*, 1995, **34**, 2225.
11 Yu. A. Simonov, M. S. Fonar', V. Kh. Kravtsov, V. O. Gel'mbol'dt, E. V. Ganin, L. O. Ostapchuk, A. A. Ennan, Yu. A. Popkov and Ya. Lipkovskii, *Zh. Neorg. Khim.*, 1998, **43**, 1982.
12 V. O. Gel'mbol'dt, Yu. A. Simonov, E. V. Ganin, A. A. Dvorkin, Ya. Lipkovski and Yu. A. Popkov, *Koord. Khim.*, 1998, **23**, 720.
13 A. L. Spek, PLATON, a Multipurpose Crystallographic Tool, Utrecht University, Utrecht, 1999.
14 A. K. Rappé, C. J. Casewit, K. S. Colwell, W. A. Goddard III and W. M. Skiff, *J. Am. Chem. Soc.*, 1992, **114**, 10024.
15 V. J. Thöm, C. C. Fox, J. C. A. Boeyens and R. D. Hancock, *J. Am. Chem. Soc.*, 1984, **106**, 5947.
16 W. Kabsch, *J. Appl. Crystallogr.*, 1988, **21**, 916.
17 N. Walker and D. Stuart, DIFABS, *Acta Crystallogr.*, *Sect. A*, 1983, **39**, 158.
18 MOLEN, Data reduction software, Enraf-Nonius, Delft, Netherlands, 1994.
19 G. M. Sheldrick, SHELXS 86, *Acta Crystallogr.*, *Sect. A*, 1990, **46**, 467; G. M. Sheldrick, SHELX 97, University of Göttingen, 1997.
20 CERIUS 2, version 3.5, Molecular Simulations Inc, San Diego, 1997.